

2021-12

# Soil erosion and sediment transport in Tanzania: Part II sedimentological evidence of phased land degradation

Wynants, Maarten

<http://hdl.handle.net/10026.1/18067>

---

10.1002/esp.5218


Earth Surface Processes and Landforms

John Wiley and Sons

---

*All content in PEARL is protected by copyright law. Author manuscripts are made available in accordance with publisher policies. Please cite only the published version using the details provided on the item record or document. In the absence of an open licence (e.g. Creative Commons), permissions for further reuse of content should be sought from the publisher or author.*

# Soil erosion and sediment transport in Tanzania: Part II – sedimentological evidence of phased land degradation

Maarten Wynants<sup>1</sup>  | Aloyce Patrick<sup>2</sup> | Linus Munishi<sup>2</sup> | Kelvin Mtei<sup>2</sup> | Samuel Bodé<sup>3</sup> | Alex Taylor<sup>1</sup> | Geoffrey Millward<sup>1</sup> | Neil Roberts<sup>1</sup> | David Gilvear<sup>1</sup> | Patrick Ndakidemi<sup>2</sup> | Pascal Boeckx<sup>3</sup> | William H. Blake<sup>1</sup>

<sup>1</sup>School of Geography, Earth and Environmental Sciences, University of Plymouth, Plymouth, UK

<sup>2</sup>Nelson Mandela African Institution of Science and Technology, Arusha, Tanzania

<sup>3</sup>Isotope Bioscience Laboratory - ISOFYS, Ghent University, Ghent, Belgium

## Correspondence

Maarten Wynants, School of Geography, Earth and Environmental Sciences, University of Plymouth, Portland Square, Drake Circus, Plymouth, PL4 8AA, UK.

Email: maarten.wynants@plymouth.ac.uk

## Funding information

Horizon 2020 Framework Programme, Grant/Award Number: 644320; UK Natural Environment Research Council, Grant/Award Number: NE/R009309/1; University of Plymouth, Faculty of Science and Engineering, PhD Scholarship; Research Council UK Global Challenges Research Fund (GCRF), Grant/Award Number: NE/P015603/1

## Abstract

Soil resources in parts of Tanzania are rapidly being depleted by increased rates of soil erosion and downstream sediment transport, threatening ecosystem health, water and livelihood security in the region. However, incomplete understanding to what effect the dynamics of soil erosion and sediment transport are responding to land-use changes and climatic variability are hindering the actions needed to future-proof Tanzanian land-use practices. Complementary environmental diagnostic tools were applied to reconstruct the rates and sources of sedimentation over time in three Tanzanian river systems that have experienced changing land use and climatic conditions. Detailed historical analysis of sediment deposits revealed drastic changes in sediment yield and source contributions. Quantitative sedimentation reconstruction using radionuclide dating showed a 20-fold increase in sediment yield over the past 120 years. The observed dramatic increase in sediment yield is most likely driven by increasing land-use pressures. Deforestation, cropland expansion and increasing grazing pressures resulted into accelerating rates of sheet erosion. A regime shift after years of progressive soil degradation and convergence of surface flows resulted into a highly incised landscape, where high amounts of eroded soil from throughout the catchment are rapidly transported downstream by strongly connected ephemeral drainage networks. By integrating complementary spatial and temporal evidence bases, this study demonstrated links between land-use change, increased soil erosion and downstream sedimentation. Such evidence can guide stakeholders and policy makers in the design of targeted management interventions to safeguard future soil health and water quality.

## KEYWORDS

climate change, East Africa, land degradation, land-use change, radiometric dating, sediment connectivity, sediment fingerprinting

## 1 | INTRODUCTION

Rates of sediment transport in Tanzania's river systems have been increasing since the 1960s (Dutton et al., 2019; Wynants et al., 2020) driven by a conjunction of increasing land-use pressures (Borrelli et al., 2017; Wynants et al., 2019) and the distinct topography and semi-arid climate (Rapp et al., 1972; Vanmaercke et al., 2014). Natural

vegetation is being progressively replaced by cropland. Moreover, while the number of livestock has increased by about 130% in the past 50 years, the areas set aside for grazing are decreasing in size, connection and quality (Wynants et al., 2019). The Food and Agriculture Organization of the United Nations (FAO, 2019) reports that in Tanzania the livestock densities on the rangelands have increased from around 20 units km<sup>-2</sup> in 1970 to 55 units km<sup>-2</sup> in 2017. The

This is an open access article under the terms of the Creative Commons Attribution License, which permits use, distribution and reproduction in any medium, provided the original work is properly cited.

© 2021 The Authors. *Earth Surface Processes and Landforms* published by John Wiley & Sons Ltd.

loss of permanent vegetation through deforestation, agricultural expansion and overgrazing drives accelerating rates of erosion, which is causing a rapid depletion of soil resources, threatening food, water and livelihood security in the region (Cobo et al., 2010; Dutton et al., 2019; Kiage, 2013; Maitima et al., 2009). Moreover, a decrease of permanent vegetation has been shown to impact surface runoff and discharge through increased seasonality with higher peak flows and lower minima (Guzha et al., 2018; Jacobs et al., 2018). Higher runoff rates have more energy to erode the surface soils and to incise the landscape where they converge (Poesen et al., 2003). Furthermore, these processes are amplified by natural rainfall variations (Ngecu & Mathu, 1999; Wynants et al., 2020) and potentially by projected increases in extreme climatic events (Borrelli et al., 2020; Shongwe et al., 2011). While soil resources are progressively being depleted, the East African population and their demand for the services the soil provides is continuing to increase (FAO, 2019; UNDESA, 2017). Continued loss of productivity and arable land would be catastrophic for the agricultural sector in Tanzania, which currently employs more than 75% of the working population, underpins the economy, and provides the basic caloric uptake for the majority of its inhabitants (FAO, 2019; Salami et al., 2010; Sanchez, 2002; Tengberg & Stocking, 1997). Besides these on-site impacts, increased downstream sediment transport also has major detrimental effects on aquatic ecosystems, water quality and energy security (Amasi et al., 2021; Olago & Odada, 2007). There is an urgent need for science-based land and water management strategies to achieve sustainable intensification of agro-pastoral production and protect soil resources. However, a lacuna in environmental data and a lack of understanding on the changing dynamics of increased soil erosion and sediment transport in Tanzania's catchments impedes the development and application of sustainable land and water management plans (Blake et al., 2018, 2020). In this context, floodplains, lakes and reservoirs are natural archives of the cumulative vertical aggradation of sediment, which record changes in sedimentation and source contributions over time (Collins et al., 1997; D'Haen et al., 2012; Hughes et al., 2009). Sediment coring, dating and fingerprinting can fill knowledge gaps and elucidate the changes in the processes of erosion and sediment transport over longer timescales than are possible via monitoring and observation (Appleby, 2008; Owens et al., 2016).

In this contribution, sediment deposits from three neighbouring Tanzanian catchments are fingerprinted using elemental geochemistry and the  $\delta^{13}\text{C}$  signature of plant-derived, long chain (> C22), saturated fatty acids (FAs). The changing contributions of different land uses, catchment zones, and erosion processes to the sediment fluxes is investigated using cluster analysis (CA) and principal component analysis (PCA). In addition to fingerprinting, the sediment deposits have also been dated radiometrically so that changes in sedimentation rates can be quantified and coupled with changes in sediment delivery dynamics. By integrating these complementary evidence bases, this study ultimately aims to elucidate the links between land use and climatic changes with the dynamics of soil erosion and sediment transport. A better understanding of the trajectory of landscape change is particularly valuable for evaluating the sustainability of current land-use practices and the design of remediation strategies that maintain and restore soil health and water quality. This publication is the second part of an article pair on soil erosion and sediment transport in Tanzania, wherein the first study focussed on quantifying

contemporary sediment source contributions in Tanzanian river systems (Wynants et al., 2021).

## 2 | MATERIAL AND METHODS

The raw dataset, model inputs, model build, and model outputs are available as open access at <https://doi.org/10.24382/9xmf-7e88>.

### 2.1 | Study sites and coring strategy

To gain a better understanding of the effects land-use and climate changes on sediment dynamics in Tanzania, three depositional areas that capture sediment from the altitude continuum were selected for sediment coring: Nanja reservoir, the Naidosoito reservoir, and the Musa floodplain (Figure 1 and Table 1). All three systems are part of the hydrologically complex Makuyuni River catchment, which is the main driver behind the increased sedimentation in Lake Manyara (Wynants et al., 2020). Results of the paired article of Wynants et al. (2021) show distinct changes in soil chemistry over an altitudinal gradient. The catchment was therefore divided in three catchment zones: up-zone [ $> 1600$  m above sea level (ASL)], mid-zone (1400–1600 m ASL), and low-zone ( $< 1400$  m ASL). Wynants et al. (2018) showed that between 1988 and 2016 over 25% of the area in the Makuyuni catchment with natural or semi-natural savannah grasslands and bushlands has been converted towards croplands or has been degraded, increasing the erosion risk in these areas. While the amount of grazing land has decreased, the number of livestock in the area has, like the rest of Tanzania, doubled in the same period, seriously increasing livestock densities and grazing pressures (FAO, 2019). The combination of these land-use changes with a natural high vulnerability to soil erosion has resulted in a marked increase in surface erosion, gully incision and land degradation in the area (Blake et al., 2018; Kiunsi & Meadows, 2006; Maerker et al., 2015). The combination of land degradation by erosion and siltation of the water bodies threatens ecosystem health and service provision in the region (Janssens de Bisthoven et al., 2020).

All three coring sites are located in what were originally natural floodplain areas, but Nanja reservoir and Naidosoito reservoir shifted towards lake systems after their river systems were dammed. The exact dates of the river damming is not known, however historical maps and records (Blake et al., 2018; Wynants et al., 2019) and information from local government officials (Kelly et al., 2020) and citizens (Rabinovich et al., 2019, 2020) indicate they were built in the 1920s by the British colonial administration in an attempt to promote water access for pastoralists. After damming, the sedimentation dynamics in Nanja reservoir and Naidosoito reservoir inevitably changed from a flood threshold-based sedimentation to a more continuous lake sedimentation. However, as is further discussed in the paired article of Wynants et al. (2021), the Makuyuni system is highly ephemeral, wherein the river discharge and flood dynamics are linked to the seasonal rainfall, which is confined to short but intensive rains. Sedimentation in the lake systems is thus also highly seasonal since most of the year there is no inflow from rivers. Furthermore, the area experiences a high inter-annual rainfall variability through the interlinking of multiple global and local climatic phenomena (Nicholson, 1996;

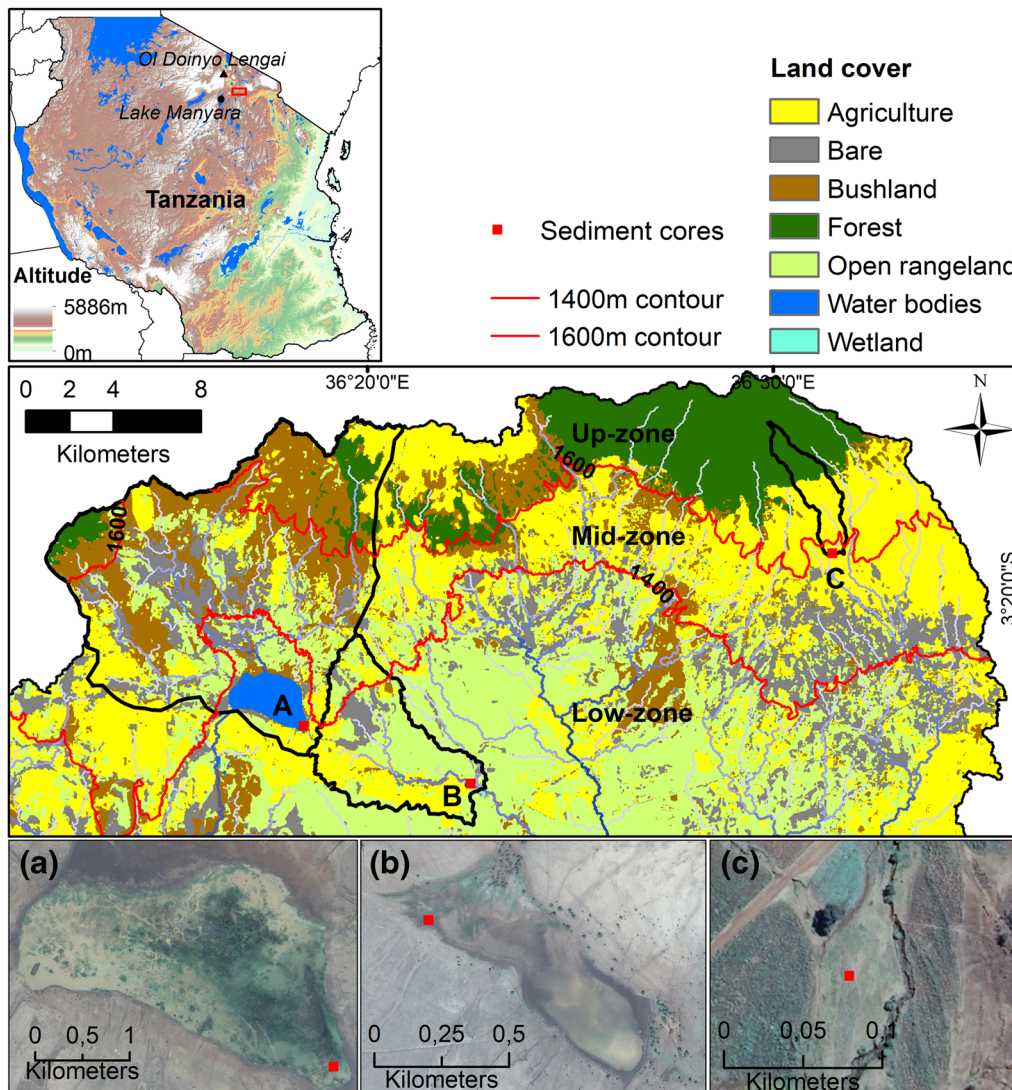


**FIGURE 1** Coring locations (red squares) and catchments of; A, Nanja reservoir; B, Naidosoito reservoir; C, Musa floodplain. The main map also depicts the dominant land cover types and the catchment zones (contour lines). The geographical context of the study site within Tanzania is given in the top left map within Tanzania, together with altitude and locations of Lake Manyara and Ol Doinyo Lengai. Below, detailed aerial photographs are given of the coring locations in (A) Nanja (image captured on January 2017, source: Google Earth), (B) Naidosoito (image captured on December 2016, source: Google Earth), and (C) Musa (image captured on August 2018, source: Google Earth)

Prins & Loth, 1988). In the drier periods when there is a prolonged lack of inflow to the reservoirs, they will not only stop receiving sediment, but will also start shrinking and often dry out completely (Deus et al., 2013).

The cores were taken from exposed sediment beds at the outer edges of the reservoirs/floodplains at locations that were submerged during the wet season (Naidosoito and Nanja) or during peak flows (Musa) but with enough distance from the high energy riverine inflow. The sediment profiles were laid out and visually screened for core stratigraphy. The monoliths and cores were subsequently wrapped in foil or polyvinyl chloride tubes and transported to the laboratory, where they were sliced at 1 cm intervals and packed for further analysis. Samples were also taken from the ash cone and mountainside of the nearby Ol Doinyo Lengai volcano (Figure 1) in order to screen them for potential geochemical markers that could be used to independently date the sediment layers.

## 2.2 | Laboratory analysis

All samples were either freeze-dried or oven-dried at 40°C and subsequently disintegrated using a mortar and pestle.

The direct determination of the  $^{210}\text{Pb}_{\text{ex}}$  activities in the Nanja and Naidosoito core sections was achieved by alpha spectrometry (Mabit et al., 2008). Due to the high labour and financial costs of alpha spectrometry, about one-third of the Naidosoito and Nanja core samples were analysed using intervals of 3 cm. The Musa core was not analysed. Radiochemical separation of  $^{210}\text{Po}$  was performed at the University of Exeter Radiometry Laboratory, UK following the protocol of Aalto and Nittroauer (2012). Samples were spiked with  $^{209}\text{Po}$  and digested with concentrated  $\text{HNO}_3$ , 30%  $\text{H}_2\text{O}_2$  and 6 M HCl (1:2:1). The digested samples were centrifuged and the supernatant was decanted into a 0.5 M HCl solution with 0.2 g ascorbic acid. Polonium isotopes were allowed to spontaneously deposit onto silver planchets suspended in the solution for 24 h. The  $^{210}\text{Po}$  and  $^{209}\text{Po}$

**TABLE 1** Characteristics of the drainage areas for each of the cored depositional features

Reservoir/floodplain	Naidosoito	Nanja	Musa
<i>Catchment characteristics</i>			
Catchment area (km <sup>2</sup> )	35	148	7.5
Elevation range (m)	1305–1506	1384–2124	1551–2256
Agriculture (%)	34.7	15.7	60.5
Bare (%)	12.8	15.6	0.0
Bushland (%)	2.7	37.9	0.2
Forest (%)	0.0	5.5	39.1
Open rangeland (%)	49.4	21.1	0.3
Wetlands (%)	0.3	0.0	0.0
Water bodies (%)	0.0	4.1	0.0
<i>Coring locations</i>			
Depositional area (km <sup>2</sup> )	0.31	5.99	0.01
Core depth (cm)	63	103	101
Date of coring	February 2017	February 2017	November 2018
Coring method	Root corer	Monolith	Monolith

alpha activities were counted using alpha spectrometers (Ortec Ultra-AS, AMETEK, Oak Ridge, Tennessee, US) for 48 to 100 h. The <sup>210</sup>Po activity determination was based on chemical recovery of the spiked <sup>209</sup>Po peak. Instrument calibration and yield determination were evaluated by comparison with <sup>210</sup>Po and <sup>209</sup>Po standard solution references supplied by the International Atomic Energy Agency (IAEA). Activities of <sup>137</sup>Cs and supported activities of <sup>210</sup>Pb were estimated by averaging <sup>214</sup>Pb activities obtained from gamma analysis of 13 core sections (Zaborska et al., 2007) using low background EG&G Ortec planar (GMX50–83-LB-C-SMN-S) and well (GWL-170-15-S) HPGe gamma spectrometers with 24 h counting times. The detectors were calibrated with a natural soil labelled with a radioactive traceable solution (80717-699, Eckert & Ziegler Analytics, Atlanta, GA, USA). Quality control was by involvement in IAEA proficiency tests of soils (IAEA-CU-2009-03; IAEA-TEL-2012-03).

All samples were analysed for major and minor element geochemistry by wavelength dispersive X-ray fluorescence (WD-XRF; OMNIAN application, Axios Max, Malvern PANalytical, Malvern, UK) using the same protocol as discussed in the paired article of Wynants et al. (2021). Prior to analysis all samples were sieved to < 63 µm to reduce particle size effects (Lacey et al., 2017; Motha et al., 2002) and because of the general focus on the detrimental fine sediment (Walling, 2013).

Compound specific stable isotope analysis (CSIA) of FAs was performed following the methodology as described in Wynants et al. (2021). Due to the high labour and financial costs of CSIA, only 26 of the 102 sediment sections of the Nanja core were selected for analysis.

## 2.3 | Data analysis

### 2.3.1 | Sediment radionuclide dating and mass accumulation rates

The Nanja and Naidosoito cores were dated and sedimentation rates were reconstructed using the constant rate of supply (CRS) model

(Appleby & Oldfield, 1978), which draws upon the rate of change in <sup>210</sup>Pb<sub>ex</sub> activity with core mass depth to derive an age–depth relationship and sediment mass accumulation rates (MARs). The half-life of <sup>210</sup>Pb ( $t_{1/2} = 22.23$  years) makes it possible to measure time-series processes up to 5–6 half-lives. Moreover, the CRS model specifically allows for changes in sedimentation rates and initial <sup>210</sup>Pb<sub>ex</sub> activity concentration in the sediment (Sanchez-Cabeza & Ruiz-Fernández, 2012), making it suitable for the purpose of this study. A detailed description of the model is given in Supporting Information Data S1. Total sediment delivery (in t yr<sup>-1</sup>) was estimated by multiplying MARs with the depositional areas. However, given the variable lake area and non-uniform MARs within the deposition areas, this estimation is likely subject to large uncertainties. Catchment sediment yield (in t km<sup>-2</sup> yr<sup>-1</sup>) was estimated by dividing the total sediment delivery per year by the total drainage area. Since the capture efficiency of the three study sites is unknown and likely variable, the sediment yield is also subject to large uncertainties on top of the uncertainties related to the estimation of the total sediment delivery. Nonetheless, the estimation of sediment yield allows a rough comparison between different river systems (Vanmaercke et al., 2014).

While the CRS model accounts for changes in lake sedimentation rates and initial <sup>210</sup>Pb<sub>ex</sub> activity, it assumes a constant rate of <sup>210</sup>Pb<sub>ex</sub> supply to the sediment (Appleby & Oldfield, 1978). This assumption might be problematic because eroded sediments from different parts of the catchments can have different <sup>210</sup>Pb<sub>ex</sub> activities due to the natural variability in the geological prevalence of <sup>238</sup>U and/or differences in dominant erosion process (He & Walling, 1997). Furthermore, changes in dominant processes of erosion within a catchment can alter the proportion of topsoil versus subsoil material in the transported sediment, thereby affecting the <sup>210</sup>Pb<sub>ex</sub> activity (Aalto & Nittrouer, 2012; Baskaran et al., 2014; Du & Walling, 2012). When the sediment delivery from the different catchment zones or erosion process varies over time, so will the secondary <sup>210</sup>Pb<sub>ex</sub> activity linked to the deposited sediment delivered to the lakes. Thus, even when the atmospheric <sup>210</sup>Pb<sub>ex</sub> flux to the lake environment stays relatively constant over time, the incoming secondary <sup>210</sup>Pb<sub>ex</sub> signature from deposited sediment might vary substantially (Appleby et al., 2019).



Normally, uncertainties due to this potential variability in  $^{210}\text{Pb}_{\text{ex}}$  fluxes can be reduced by fitting the model to the independent  $^{137}\text{Cs}$  southern hemisphere 1965 peak fallout (Appleby, 2008). However, due to low  $^{137}\text{Cs}$  fallout in tropical Africa (Walling & He, 2000), the CRS-fitted approach might be counterproductive and even increase the uncertainty in sediment dating (Appleby et al., 2019). This prohibited the correction of errors related to the potential variations in rate of  $^{210}\text{Pb}_{\text{ex}}$  supply. Therefore, the geochemical profiles of the cores were also scanned for distinct changes or peaks that could be linked to known hydrological (Łokas et al., 2010; Wynants et al., 2020) or volcanic (Arnaud et al., 2006) events.

### 2.3.2 | Core fingerprint analysis

The elemental geochemical records from all cores and  $\delta^{13}\text{C}$ -FA record from the Nanja core was subject to PCA and CA to draw out evidence for shifts in sediment source and processes of erosion (D'Haen et al., 2012; Owens et al., 2016). On the PCA biplot, the direction of the tracer vectors was compared with the observed depth profile trends. In addition to the multivariate analysis, the relative changes in processes and sources of erosion were explored using depth profile analysis on the individual tracers. Tracers for the core PCA were thus evaluated on the strength and direction of their signal. In order to make conclusions about what the observed increased importance of certain tracers indicated, the geochemical and  $\delta^{13}\text{C}$ -FA soil continuum from the entire northern Makuyuni region was consulted. The detailed methodology and outputs from this soil fingerprinting can be found in the paired article (Wynants et al., 2021). This way, geochemical or biochemical trends found in the core could be linked to changing contributions from certain source zones, processes and/or land-use types in the catchment (Lizaga et al., 2019, 2021). In addition, the wider literature around soil chemistry and environmental carbon isotopic trends, as well as the post-depositional behaviour in sediments was consulted. Basic range tests between soil sources and the cores (Supporting Information Figures S1–S4) were used to screen individual tracers for fluvial sorting processes (Belmont et al., 2014; Sherriff et al., 2015). The selected tracers for the core PCA can be found in Supporting Information Table S1.

Allogenic tracers are associated with hillslope soils, where they are produced through location-specific pedological weathering processes (Schillereff et al., 2014). Autogenic tracers are associated with production within lakes and floodplains. In this semi-arid context, this mostly takes place through the precipitation of solutes as salts in evaporating water bodies (Jones & Deocampo, 2003). Increased concentrations of allogenic tracers in the sediment column signal a higher proportional contribution of eroded hillslope soils, while higher concentrations of autogenic tracers signal lower rates of sediment delivery from the catchment (Owens et al., 2016; Wynants et al., 2020). Within allogenic tracers, a distinction can be made on whether the eroded sediment comes from the soil surface, or from deeper subsurface layers. Surface tracers are elements that are generally concentrated in the soil surface through environmental processes (Du & Walling, 2017) and can in turn also be classified into two subgroups: evaporative and detrital tracers. Evaporative tracers can become concentrated in the upper soil layers, mostly in drier and hotter lowland areas, due to higher rates of water output by evaporation over water

input by precipitation/runoff (Allison & Hughes, 1983). The detrital tracers are associated with soil organic matter and are often concentrated in the upper soil layers because these layers have the highest biological input and activity. However, since most Tanzanian catchments have a distinct rainfall and vegetation gradient in the catchment, the detrital tracers are also often linked to the up-zone soils, where higher rainfall allows more vegetation growth and more biological input in the soil (Wynants et al., 2021). Increased contribution of these detrital tracers thus usually signals higher proportional contribution of up-zone surface soils. Subsurface tracers are elements that have higher concentrations in deeper soil layers (Manjoro et al., 2017). Often these tracers are more resistant to weathering or are less weathered and thus are assumed to originate closer to the bedrock. Higher concentrations of the elements tend to signal a higher proportional contribution of subsurface gully or riverine erosion close to the bedrock. Since  $\delta^{13}\text{C}$ -FA signature in soils is solely dependent on the biological input in the soil, they can be used as land-use tracers. The  $\delta^{13}\text{C}$ -FA fingerprint in plants is mainly driven by the altitude-rainfall gradient, working through the C3/C4 metabolic pathway and altitude effects on the plant  $\delta^{13}\text{C}$  signal (Lizaga et al., 2021; Upadhayay et al., 2020). In general, woody C3 plants with lower  $\delta^{13}\text{C}$  dominate the wetter up-zone, while grassy C4 plants with higher  $\delta^{13}\text{C}$  values dominate the drier low-zone (Osborne, 2008). As maize is a C4 plant, soils under the dominant maize cropping systems will also incorporate a C4 signal (Christensen et al., 2011).

Observed trends in the geochemical profile are not always solely due to changes in the delivered sediment. Post-depositional diagenetic processes can potentially also influence the observed core profiles (Outridge & Wang, 2015). Wave activity and biological activity in the lakes could lead to resuspension and mixing of the upper sediment layers. Moreover, the periodic drying of a lake exposes the surface of the sediment deposit to the wind and other forces, potentially leading to post-depositional removal or mixing. Furthermore, this periodicity in lake levels could influence redox conditions and therefore could have an effect on the mobility of some metals. However, for this specific Tanzanian setting, the effects of physical mixing and post-depositional erosion are probably negligible because of the high clay content of the sediment that facilitates the formation of strong aggregates during drying that are too heavy to be removed by wind erosion. Moreover, coincidence of high lake levels with dynamic flow conditions and rainfall events mean the lakes are well oxygenated during their highest levels. Additionally, due the high clay content, the metals are less likely to move vertically in the core profile because they will be bound very strongly to the sediment particles. The dense clay layering also has very low infiltration rates and therefore does not promote porewater transport.

## 3 | RESULTS

### 3.1 | Sedimentation reconstruction

All cores were dominated by heavy clay sediments and had no visible stratigraphy. Figure 2 shows the measured  $^{210}\text{Pb}_{\text{ex}}$  profiles and modelled MARs of the Naidosoito (Figure 2a,c, respectively) and the Nanja (Figure 2b,d, respectively) cores. Both cores had two distinct peaks in  $^{210}\text{Pb}_{\text{ex}}$  activity and all  $^{137}\text{Cs}$  activities were below the limit of

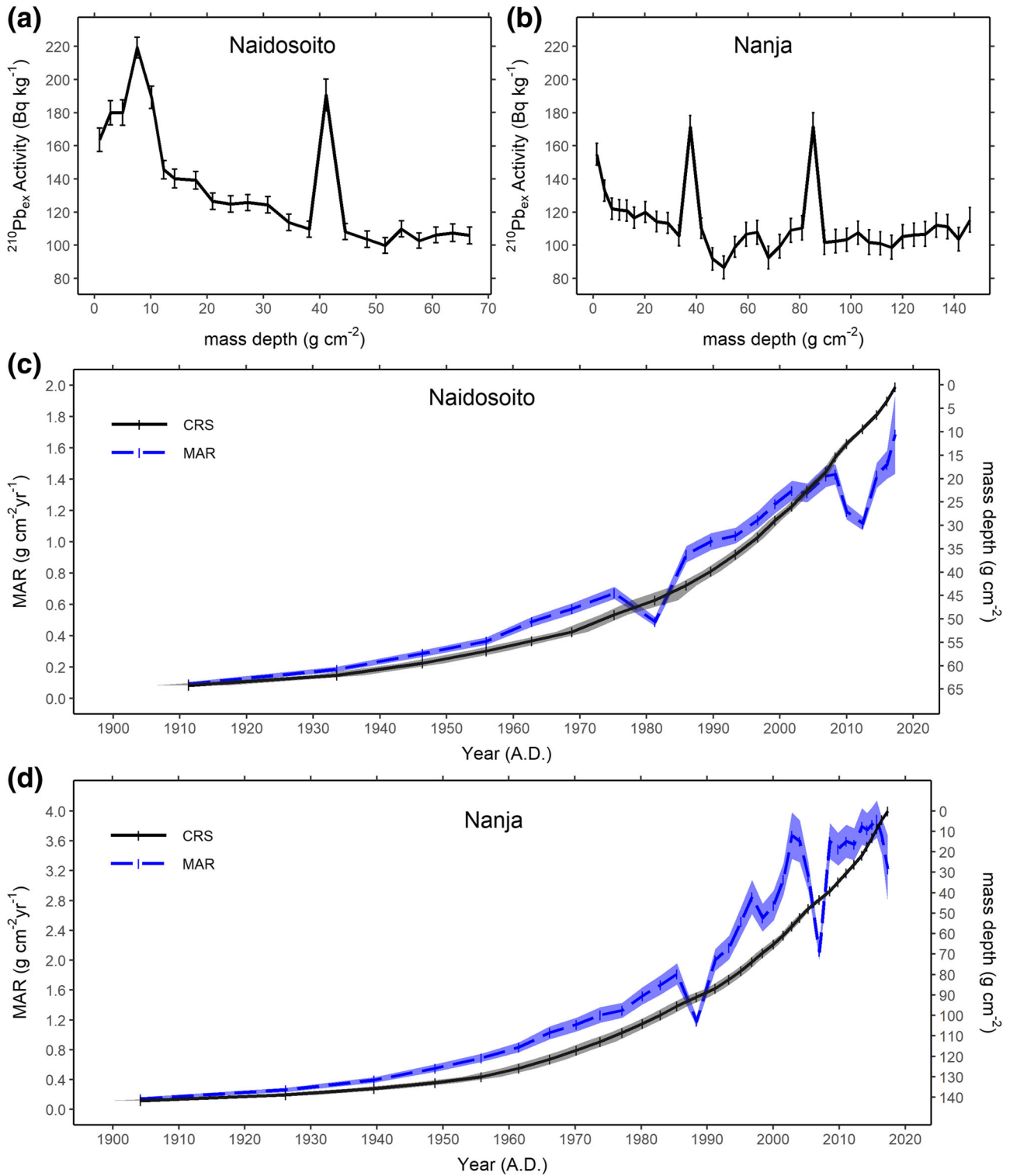


**FIGURE 2** The  $^{210}\text{Pb}_{\text{ex}}$  profiles of the Naidosoito (a) and Nanja (b) cores with analytical error bars. The constant rate of supply age–mass depth profile (CRS, full black line) with standard deviation intervals (grey) and the mass accumulation rates (MARs, dashed blue line) with standard deviation intervals (blue) of the Naidosoito (c) and Nanja (d) cores

detection. The mean  $^{214}\text{Pb}$  activity measured by gamma spectrometry was  $18.94 \text{ Bq kg}^{-1}$ , ranging between  $14.85 \text{ Bq kg}^{-1}$  and  $22.49 \text{ Bq kg}^{-1}$ . The CRS model output shows similar trends for both cores and dated the penultimate deepest sections to the beginning of the 20th century. By assuming a continuation of the CRS profile, the age of the deepest core sections could be estimated to be around 1875 for both cores. Reconstruction of the MAR rates in both the Naidosoito core (Figure 2c) and Nanja core (Figure 2d) show an exponential increase in

sedimentation. The MAR increase in Naidosoito is nearly 20-fold from  $0.09 \text{ g cm}^{-2} \text{ yr}^{-1}$  in 1912 to  $1.69 \text{ g cm}^{-2} \text{ yr}^{-1}$  in 2017 and in Nanja it is nearly 30-fold from  $0.14 \text{ g cm}^{-2} \text{ yr}^{-1}$  in 1903 to  $3.95 \text{ g cm}^{-2} \text{ yr}^{-1}$  in 2015. Converted to catchment-specific sediment yield, this amounts to an increase from 8 to  $149 \text{ t km}^{-2} \text{ yr}^{-1}$  in the lower-sloped Naidosoito drainage area and from 57 to nearly  $1600 \text{ t km}^{-2} \text{ yr}^{-1}$  in the larger and more diverse Nanja drainage area. In both cores, two distinct drops in MAR can be observed, for Naidosoito in 1981 and

2009–2012, while for Nanja in 1988 and 2006. In both cases, the drops are to rates that are still much higher than in older sections.

## 3.2 | Sediment core fingerprint analysis

### 3.2.1 | Naidosoito core

The main trend in the core (Figures 3 and S5) is an increase in importance of the some of the allogenic hillslope tracers (Ti, Fe<sub>2</sub>O<sub>3</sub>, Al<sub>2</sub>O<sub>3</sub>, Zn, ...) and a linked decrease in the autogenic tracers (K<sub>2</sub>O, Na<sub>2</sub>O, MgO and Sr). The core evidences a long-lasting stability in sediment sources between 1875 and 1987. The sediment deposited in this period is characterized by higher concentrations of subsurface tracers (SiO<sub>2</sub> and Rb) and autogenic tracers (MgO, Na<sub>2</sub>O and K<sub>2</sub>O) around 1900, the 1960s and recently, while in between the concentration remains more or less stable around 180 ppm.

A distinct shift is recorded from c. 1990 onwards and seems to indicate increasing importance of topsoil contribution to the reservoir evidenced by P<sub>2</sub>O<sub>5</sub>, SO<sub>3</sub>, Ti, Nb, Y, Ba, CaO and Mn. This situation of increased surface contribution remained stable for about 20 years, after which the core records a rapid shift characterized by a weathering signal: Fe<sub>2</sub>O<sub>3</sub>, Zr, Zn, Ni, Y and Al<sub>2</sub>O<sub>3</sub>. The Ce profile evidences very distinct peaks in concentration up to 1100 ppm

### 3.2.2 | Nanja core

The main observed trend in the Nanja core (Figures 4 and S6) is a decreasing concentration of autogenic tracers (MgO, Sr, F, Na<sub>2</sub>O), combined with an increase in concentration of allogenic hillslope elements (Ti, P<sub>2</sub>O<sub>5</sub>, SO<sub>3</sub>, Fe<sub>2</sub>O<sub>3</sub>, Nb). As in the Naidosoito core, the oldest core sections are characterized by higher concentrations of SiO<sub>2</sub> and

Rb, indicating a higher relative importance of bedrock incision processes. From the 1960s, the core records gradually increasing concentrations of CaO, Ba, Co and Mn, and lower concentrations of SiO<sub>2</sub>, Rb and Al<sub>2</sub>O<sub>3</sub>, indicating a shift to increasing contribution of topsoil. This situation remained until c. 2004, while experiencing a parallel increase in allogenic sediment delivery. From 2005 onwards, the core records a jump back to increasing levels of SiO<sub>2</sub>, Rb and Al<sub>2</sub>O<sub>3</sub>, which is followed by rapid increases in Ti, P<sub>2</sub>O<sub>5</sub>, SO<sub>3</sub>, Fe<sub>2</sub>O<sub>3</sub> and Nb. This indicates increasing bedrock and hillslope gully incision that rapidly funnel eroded hillslope soils downstream through the increasingly connected landscape. The Ce profile in Nanja also evidences very distinct peaks in concentration, albeit to slightly lower concentrations and on slightly different times (around 600 ppm in 1880 and 1960, and up to 1100 ppm in 2000).

Analysis of the Nanja core  $\delta^{13}\text{C}$ -FA profiles (Figure S8) and PCA plot (Figure 5) evidence distinct historical shifts in contributions from soils of different land-use types to the sediment. The oldest sections of the Nanja core take a central position on the PCA plot, indicating a relative balance between sediment contribution from the drier mid-zone and wetter up-zone. From 1958 to 1985 the core records a distinct drop in  $\delta^{13}\text{C}$ -FA, indicating an increase in the contribution from the up-zone forest and bushland with a peak in 1961. From 1991 to 2012, the core sways to increased  $\delta^{13}\text{C}$ -FA, indicating increased contribution from the drier low-zone. Interestingly, the most recent core sections (2014–2017) point towards a subsequent higher contribution of wetter upland soils, albeit to lesser extent than the 1958–1985 section.

### 3.2.3 | Musa core

The multivariate PCA plot and elemental profiles of the Musa core are shown in Figures 6 and S7, respectively. Like the other cores, the main observable trend is decreasing concentrations of autogenic tracers

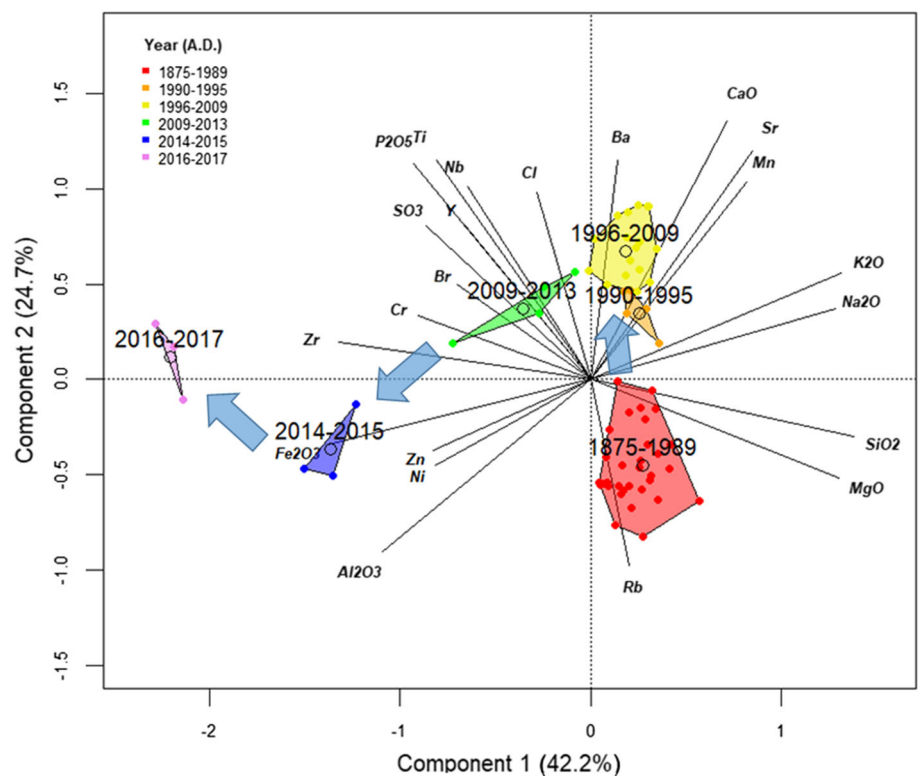


**FIGURE 3** PCA plot of the Naidosoito core visualizing changes in geochemical fingerprint over time, related to changing dynamics of soil erosion and sediment transport. Coloured areas are the hull areas around the core clusters with the centroid drawn as hollow circle. Arrows indicate direction of change over time. The core PCA with raw data points can be found in Supporting Information Figure S10



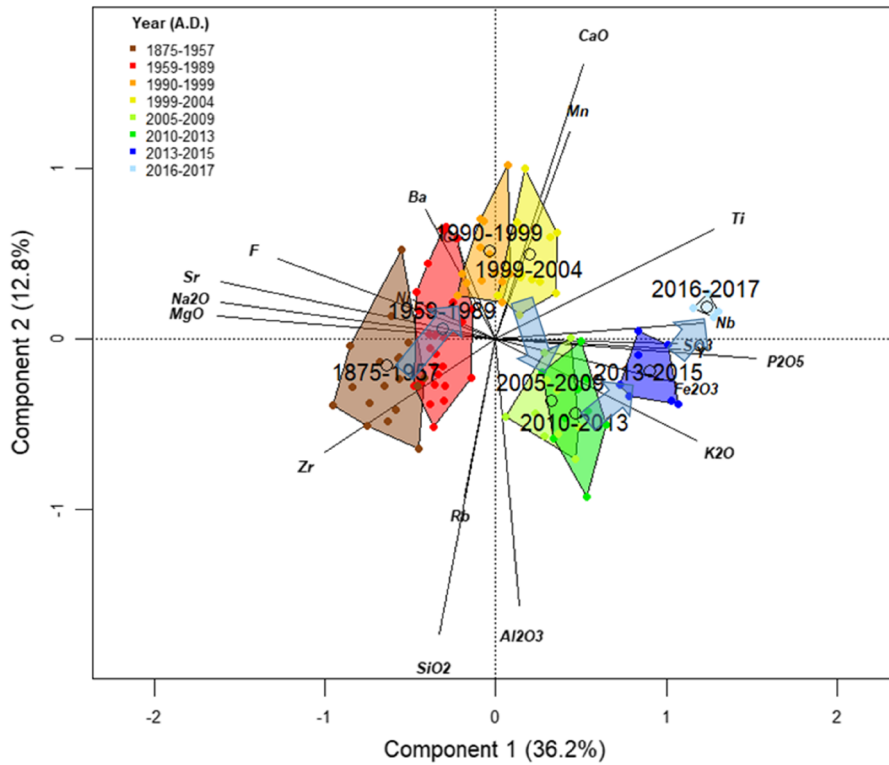


**FIGURE 4** The geochemical Nanja core PCA plot. Coloured areas are the hull areas around the core clusters with centroid drawn as hollow circle. Arrows indicate direction of change. The core PCA with individual dates can be found in Supporting Information Figure S11

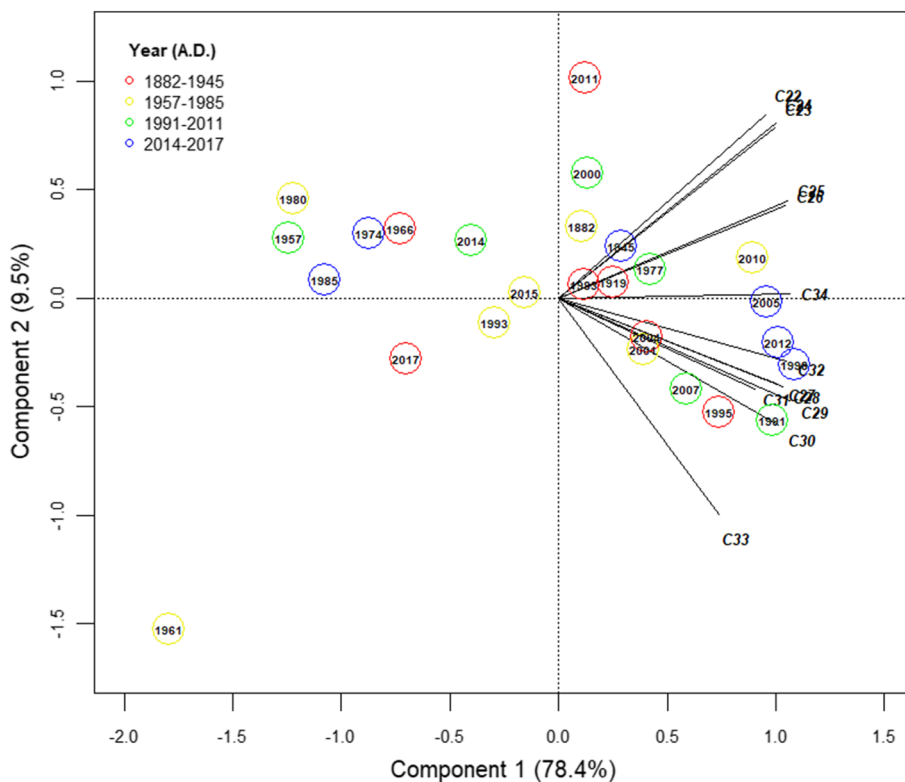
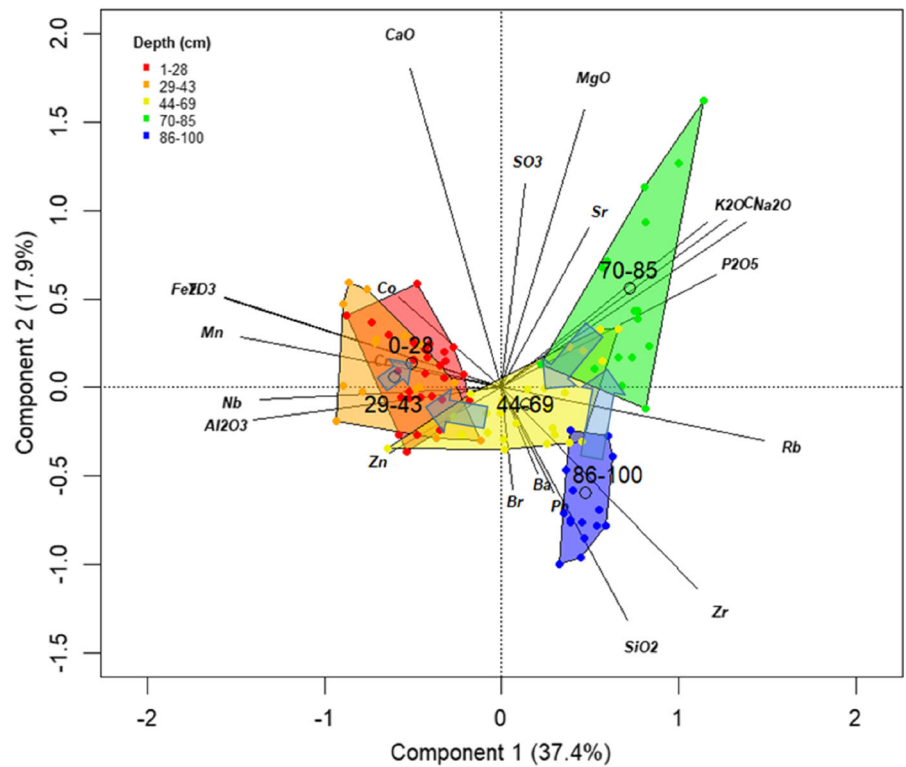


**FIGURE 5** The  $\delta^{13}\text{C}$ -FA PCA plot of the Nanja sediment core, wherein the C-number indicates the amount of carbons of the specific fatty acids (FAs)

( $\text{Na}_2\text{O}$ , Cl, and  $\text{K}_2\text{O}$ ) and increasing concentrations of allogenic hillslope tracers ( $\text{Fe}_2\text{O}_3$ , Ti, Mn, Nb,  $\text{Al}_2\text{O}_3$ ) and thus seems to be related to increasing rates of sediment delivery. Moreover, the deepest sections of the Musa core are also characterized by a  $\text{SiO}_2$  and Rb signal that indicates an original higher proportional contribution of bed incision erosion. The core subsequently records a punctuated detrital signal (70–85 cm) with increased concentrations of  $\text{SO}_3$ , CaO and  $\text{P}_2\text{O}_3$ , that indicate increased contribution of up-zone forest topsoils following deforestation.

From 70 cm depth the core gradually shifts towards increasing importance of  $\text{Fe}_2\text{O}_3$ , Ti, Mn, Nb and  $\text{Al}_2\text{O}_3$ , pointing towards a general increase in hillslope erosion rates and downstream sediment delivery. However, this could also indicate incision into deeply weathered soils and/or continued erosion of already topsoil depleted soils. Moreover, some of the deeper core sections lie further on the axis than expected, possibly marking distinct high erosion events. Similarly to both other cores, the Ce profile in Musa also evidences very

**FIGURE 6** PCA plot visualizing geochemical trends with depth in the Musa core. Coloured areas are the hull areas around the core clusters with centroid drawn as hollow circle. Arrows indicate direction of change. The core PCA with raw data points can be found in Supporting Information Figure S12



distinct peaks in concentration, albeit most of them to c. 600 ppm and only the top of the core to c. 1100 ppm.

#### 4 | DISCUSSION

Low rates of  $^{137}\text{Cs}$  deposition in the southern hemisphere (Appleby, 2002) prohibited the correction of errors related to the potential variations in rate of  $^{210}\text{Pb}_{\text{ex}}$  supply. While spatial variations are probably minor due to the relatively small drainage areas, changing contributions of subsurface soils would have influenced the CRS-model, adding some uncertainty to the results. Moreover, estimating supported  $^{210}\text{Pb}$  by averaging activities of  $^{214}\text{Pb}$  obtained by gamma analysis, might not capture the full variation in  $^{210}\text{Pb}_{\text{ex}}$  activities (Zaborska et al., 2007). However, the explicit output from the model means that potential variations in the rate of  $^{210}\text{Pb}_{\text{ex}}$  supply would not have changed the observed trend of exponentially increasing sedimentation (Appleby, 2008; Sanchez-Cabeza & Ruiz-Fernández, 2012). More importantly, the increasing concentrations of allogenic tracers and decreasing concentrations of autogenic tracers found in the Nanja and Naidosoito cores, indicate an increasing input of terrestrial soils to the lake sediment as shown by Wynants et al. (2020) on Lake Man-yara. Lake shore erosion is not likely to be an explanation for the observed trends since the reservoirs have no clear lake shore and wave action is minimal. Moreover, if lake shore erosion would be a major driver of increased sedimentation, we would expect to see opposite trends to the ones visible in the cores now. Both CRS modelling and core fingerprinting thus independently confirm the increasing sediment transport to the Naidosoito reservoir and Nanja reservoir. MAR reconstruction was not done on the Musa core as no  $^{210}\text{Pb}_{\text{ex}}$  dating was performed on its core. However, similar to the Nanja and Naidosoito cores, the Musa core shows an increase in concentration for the allogenic tracers (Figure S7), indicating increasing rates of

sediment delivery from upstream hillslope sources. The distinct Ce profile in all cores might be related to periodic ash deposits from the nearby Ol Doinyo Lengai volcano (Balashova et al., 2018). Analysis of soil samples from the ash cone of the volcano yielded Ce concentrations similar to those in the peaks in the sediment cores (Figure S9). While more research will be needed to link this geochemical peak to volcanic eruptions, these results already provide a promising lead in the search for independent time markers that can improve the accuracy of sediment dating models in East Africa.

The sediment yield values are about 10-fold higher in the Nanja drainage area compared to Naidosoito, which is probably due to the more accentuated terrain. The small differences ( $\pm 4$  years difference) in age of the MAR drops between the Naidosoito and Nanja core may be due to uncertainties related to the  $^{210}\text{Pb}_{\text{ex}}$  dating, or due to sub-catchment differences. Nonetheless, the drops seem to correlate to some extent with recorded droughts (Figure 7), providing evidence of drought-related drops in soil erosion rates and sediment transport. However, if rainfall were to be the ultimate driver of the increased erosion and sediment transport, a more punctuated MAR profile would be expected. The lack of seasonality in MAR can be partly explained by the depth intervals of 1 cm that, especially in the deeper core section, might include multiple years. Moreover, wave action (when wet), wind erosion (when dry) and biological activity could also have mixed the upper sediment layers, buffering sediment dating at the scale of years. Nonetheless, the exponential increase in sedimentation rates of both reservoirs can only be explained by gradually accelerating rates of soil erosion and downstream sediment transport.

Analysis of tracer core profiles and multivariate tracer ordination allowed the evaluation of changing landscape dynamics in the three sub-catchments. While certain tracers can be linked to specific origins and dynamics of sediment delivery, it is important to note that single tracers can represent multiple signals and that soil chemistry has a large spatial variance due to localized pedological processes (Wynants

### Timeline of soil erosion and sediment transport in Tanzania

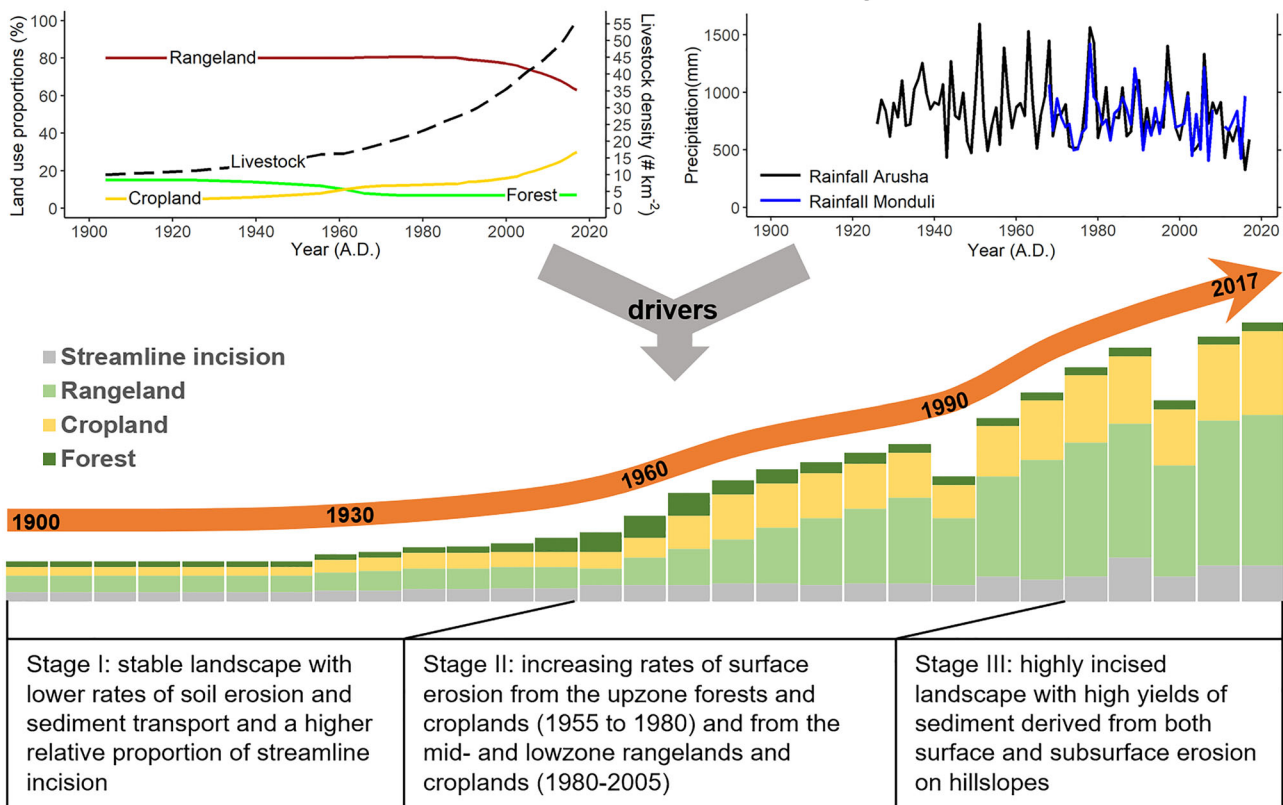


**FIGURE 7** Overview figure depicting the trajectory of land degradation in Tanzania driven by the interaction of land-use changes and rainfall variability. The changes in land use and livestock densities were estimated from previous studies (Wynants et al., 2018) and data from FAO (2019). Yearly changes in annual precipitation (mm) are based on measurements from the Selian Agricultural Research Institute, Arusha, altitude: 1402 m, coordinates: 03°21'52" S 36°38'6" E (black) and the District Agricultural Office, Monduli town, altitude: 1551 m, coordinates: 03°17'52.48" S 36°26'44.82" E (blue)

et al., 2021). Evaporative tracers can, for example, both signal lower rates of sediment delivery and increased proportional contribution of the low-zone of catchments. Subsurface erosion in deeply weathered soils can increase the proportional contribution of weathering tracers due the lack of dilution by detrital or evaporative tracers. This convolution of sediment tracers complicates the evaluation of core trends, which should always be complemented by contextual data on the catchment systems.

Nonetheless, the remarkable similarity in all three cores provides strong evidence of regional landscape change, which is underpinned by aerial photographs (Figure 8), land-use and land-cover data (Blake et al., 2020; FAO, 2019; Wynants et al., 2018), climatological evidence (Figure 7), oral narratives (Blake et al., 2018; Rabinovich et al., 2019) and historical evidence (Kelly et al., 2020; Wynants et al., 2019). The main trend in all three cores is an increase in the concentration of allogenic tracers, which relates to increasing rates of upstream soil erosion and sediment delivery. Moreover, in all cores, the older sections record a long period of relative stability characterized by a higher proportional contribution of bedrock sediment sources. However, the timing of the onset and the dynamics of the recorded changes appear to have been slightly different for each of the cores.

In the Nanja core, linking sedimentation reconstruction with geochemical and biochemical analyses paints a complex history of landscape change. Increased sediment delivery to Nanja reservoir during the late 1950s and 1960s seems to originate from the wetter up-zone

surface soils and is probably linked to deforestation and abandonment of soil conservation practices (Figure 9) in the 1960s after independence, as described in Conte (1999). From the 1980s the continued increase in sediment delivery mostly originates from the mid-zone and low-zone caused by conversion of savannah grasslands to maize cropland and progressively increasing grazing pressures on the remaining grasslands (Figure S13).

A punctuated increase in subsurface tracers from 2005 followed by a further increase in allogenic hillslope tracers points towards a regime shift where the gradual weakening of the soils combined with a high rainfall period rapidly incised the landscape through gully formation. Because most of the remaining forest has been protected and remained stable since the 1980s (Wynants et al., 2018), the latest increase in upland soil contribution is likely due to the higher connectivity between the up-zone and the river network through the recent gully incision, where high amounts of eroded soils from all catchment zones are rapidly transported downstream.

The Naidosoito core only captures the mid- to low-zone of the catchment and only evidences major changes from the 1990s with an increased relative importance of topsoil contribution for about 20 years (Figure S13). This finding relates to increasing land-use pressures in Tanzania by cropland expansion and overgrazing, and corresponding rates of surface erosion (FAO, 2019; Wynants et al., 2018). From 2009 onwards, the core evidences a distinct increase in weathering tracers, which likely signals an acceleration in

**FIGURE 8** Hillslope terrace collapse after abandonment of agricultural soil conservation practices (latitude:  $-3.344074^\circ$ , longitude:  $36.521724^\circ$ )

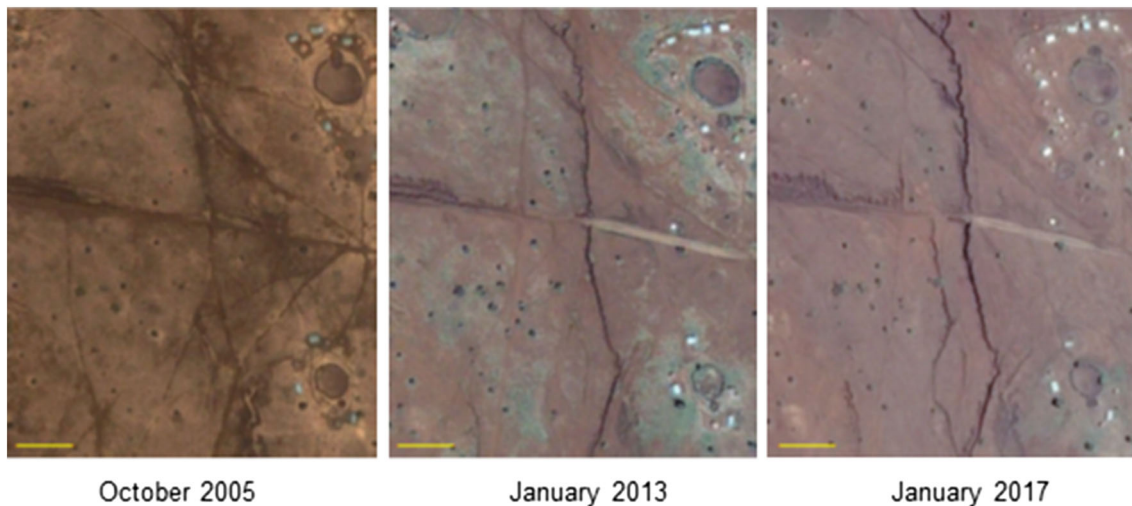


**FIGURE 9** Repeated aerial photography showing recent rapid gully incision and hillslope progression (latitude:  $-3.334067^\circ$ , longitude:  $36.360801^\circ$ ). A ground photograph of the gully in 2017 can be found in Supporting Information Figure S14. The yellow line corresponds with 50 m (source: Google Earth)

hillslope degradation through surface incision that both increases the direct contribution of deeper soil layers and rapidly funnels eroded sediment further downstream (Blake et al., 2020). This indication of rapid gully onset after a longer period of increasing contribution from topsoils is observed in both Nanja and Naidosoito, wherein the former it seems to start around 2005 and in the latter in 2009. This timeline strongly corroborates with oral (Blake et al., 2018; Kelly et al., 2020; Rabinovich et al., 2019) and aerial photographic (Figure 8) records of gully incision in the landscape (Blake et al., 2020).

In 2006, a very wet year followed a 3-year dry period (Figure 7), which could have been the climatic straw that broke the landscape's back, wherein the conjunction of drought and unsustainable land use stripped the landscape of much of the vegetation during the dry period. The exposed soils were subsequently more vulnerable to erosion and lacked the buffering capacity, leading to extreme levels of runoff and erosion during the intense 2006 rainy season. The landscape incision further sped up the loss of water and soil material from

hillslopes, leading to lateral and uphill gully progression and ultimately badland formation (Figures 10, S14 and S15). The slight differences in the timing for both cores lie within the previously discussed uncertainties around the  $^{210}\text{Pb}_{\text{ex}}$  dating.

Conversely to Naidosoito, the Musa floodplain only captures the wetter up-zone and evidences a punctuated deforestation driven increase in allogenic sediment delivery followed by continued elevated sediment delivery originating from farmed surface hillslope soils. Because no  $^{210}\text{Pb}_{\text{ex}}$  dating was performed on the Musa core, it is not possible to couple its geochemical trends with specific time periods. However, it is highly likely that similar to the Nanja system the onset of changes corresponds with the early 1960s period of uncontrolled deforestation. Overall, the recorded changes in the Musa core are less distinct compared to the Naidosoito and Nanja cores. This can be partly explained by the smaller drainage area (Table 1), but also by the more widespread soil conservation practices on the croplands in the Musa up-zone (Figure S16).





**FIGURE 10** Degraded hillslope that has turned into badland (latitude:  $-3.339357^{\circ}$ , longitude:  $36.354331^{\circ}$ )

The common trend in all cores is the continuous increase in sediment yield. Closer inspection of the sedimentary record revealed a trajectory of landscape development in three stages with, (1) an initial stable state of low erosion rates and with a higher relative importance of streamline incision-sediment sources up until  $\sim 1955$ , (2) a subsequent stage of increasing sediment yields linked to increased surface erosion in the up-zone catchment ( $\sim 1955$  to  $\sim 1980$ ) and from the mid- and low-zone catchment ( $\sim 1980$  to  $\sim 2005$ ), and (3) a current stage of a highly connected landscape with very high yields of sediment derived from both surface and gully erosion (post-2005). This final stage is further elaborated by the outcomes of the paired article of Wynants et al. (2021) that attributed most of the riverine sediment to hillslope erosion on the rangelands and maize croplands in the catchment mid-zone.

## 5 | CONCLUSION

The integration of  $^{210}\text{Pb}_{\text{ex}}$  dating, geochemical and biochemical fingerprinting greatly improved the understanding of the highly complex historical landscape dynamics in northern Tanzanian catchments. Results from these complementary diagnostic tools evidenced drastic changes in the soil erosion and sediment transport dynamics over the past 120 years. The observed evidence of phased land degradation seems to be caused by an interaction between increasing land-use pressures and climatic variability. The progressive removal of the natural vegetation by forest degradation, overgrazing and cropland expansion have greatly reduced the natural resilience of the soil system to buffer against climatic events [e.g., El Niño Southern Oscillation (ENSO)-related]. Hillslope soils, weakened by topsoil erosion and a lack of soil organic matter content, rapidly incised during extreme rainfall events. This incision further sped up the removal of water and soil material from hillslopes often leading them to evolve into badlands and resulting into a dramatic increase in catchment sediment yields.

In the context of the major global and regional challenges ahead, future research on soil erosion and sediment yield should focus on further elucidating these synergies between Land-Use and Cover-Change (LUCC) project and changing rainfall dynamics as drivers of both upstream hillslope erosion and downstream sediment propagation. A better understanding is needed of the role of gully incision, not only as a source of sediment, but also as a positive feedback loop in the processes of land degradation and sediment connectivity. While more research is needed, the gravity of the problem also requires immediate action to reduce soil erosion and downstream sediment transport. The presented trajectory of land degradation can guide Tanzanian land users and land managers in implementing the necessary steps for mitigating soil degradation and landscape incision.

## ACKNOWLEDGEMENTS

This work was carried out as part of a PhD project funded by University of Plymouth, Faculty of Science and Engineering, PhD Scholarship with additional support from the European Commission (Horizon 2020 IMIXSED project ID 644320), the Research Council UK Global Challenges Research Fund (GCRF) grant NE/P015603/1 and UK Natural Environment Research Council Grant NE/R009309/1. The authors would also like to extend their gratitude to the wider research community at the Nelson Mandela Institution for Science and Technology in Arusha, Tanzania for their guidance and logistical support during the field campaigns. Finally, the authors would like to thank the reviewers for their suggestions and feedback that have improved the quality of the publication.

## CONFLICT OF INTEREST

The authors have no conflict of interest to declare.

## DATA AVAILABILITY STATEMENT

The raw dataset, model inputs, model build and model outputs are available open access on <https://doi.org/10.24382/9xmf-7e88>.



## ORCID

Maarten Wynants  <https://orcid.org/0000-0002-5367-7619>

## REFERENCES

- Aalto, R. & Nittrouer, C.A. (2012) 210 Pb geochronology of flood events in large tropical river systems. *Philosophical Transactions of the Royal Society a: Mathematical, Physical and Engineering Sciences*, 370(1966), 2040–2074. <https://doi.org/10.1098/rsta.2011.0607>
- Allison, G. & Hughes, M. (1983) The use of natural tracers as indicators of soil-water movement in a temperate semi-arid region. *Journal of Hydrology*, 60(1-4), 157–173. [https://doi.org/10.1016/0022-1694\(83\)90019-7](https://doi.org/10.1016/0022-1694(83)90019-7)
- Amasi, A., Wynants, M., Blake, W. & Mtei, K. (2021) Drivers, impacts and mitigation of increased sedimentation in the hydropower reservoirs of east Africa. *Land*, 10(6), 638. <https://doi.org/10.3390/land10060638>
- Appleby, P. (2002) *Chronostratigraphic techniques in recent sediments. Tracking environmental change using lake sediments*. Berlin: Springer 10.1007/0-306-47669-X\_9.
- Appleby, P.G. (2008) Three decades of dating recent sediments by fallout radionuclides: A review. *The Holocene*, 18(1), 83–93. <https://doi.org/10.1177/0959683607085598>
- Appleby, P.G. & Oldfield, F. (1978) The calculation of lead-210 dates assuming a constant rate of supply of unsupported 210Pb to the sediment. *Catena*, 5(1), 1–8. [https://doi.org/10.1016/S0341-8162\(78\)80002-2](https://doi.org/10.1016/S0341-8162(78)80002-2)
- Appleby, P., Semertidou, P., Piliposian, G., Chiverrell, R., Schillereff, D. & Warburton, J. (2019) The transport and mass balance of fallout radionuclides in Brotherswater, Cumbria (UK). *Journal of Paleolimnology*, 62(4), 389–407. <https://doi.org/10.1007/s10933-019-00095-z>
- Arnaud, F., Magand, O., Chapron, E., Bertrand, S., Boës, X., Charlet, F. & Mélières, M.A. (2006) Radionuclide dating (210Pb, 137Cs, 241Am) of recent lake sediments in a highly active geodynamic setting (Lakes Puyehue and Icalma—Chilean Lake District). *Science of the Total Environment*, 366(2-3), 837–850. <https://doi.org/10.1016/j.scitotenv.2005.08.013>
- Balashova, A., Mattsson, H.B. & Hirt, A.M. (2018) New tephrostratigraphic data from Lake Emakat (northern Tanzania): Implications for the eruptive history of the Oldoinyo Lengai volcano. *Journal of African Earth Sciences*, 147, 374–382. <https://doi.org/10.1016/j.jafrearsci.2018.06.033>
- Baskaran, M., Nix, J., Kuyper, C. & Karunakara, N. (2014) Problems with the dating of sediment core using excess 210Pb in a freshwater system impacted by large scale watershed changes. *Journal of Environmental Radioactivity*, 138, 355–363. <https://doi.org/10.1016/j.jenvrad.2014.07.006>
- Belmont, P., Willenbring, J.K., Schottler, S.P., Marquard, J., Kumarasamy, K. & Hemmis, J.M. (2014) Toward generalizable sediment fingerprinting with tracers that are conservative and non-conservative over sediment routing timescales. *Journal of Soils and Sediments*, 14(8), 1479–1492. <https://doi.org/10.1007/s11368-014-0913-5>
- Blake, W.H., Kelly, C., Wynants, M., Patrick, A., Lewin, S., Lawson, J. et al. (2020) Integrating land-water-people connectivity concepts across disciplines for co-design of soil erosion solutions. *Land Degradation & Development*, 32(12), 3415–3430. <https://doi.org/10.1002/ldr.3791>
- Blake, W.H., Rabinovich, A., Wynants, M., Kelly, C., Nasser, M., Ngondya, I. et al. (2018) Soil erosion in East Africa: an interdisciplinary approach to realising pastoral land management change. *Environmental Research Letters*, 13(12), 124014. <https://doi.org/10.1088/1748-9326/a8a8b>
- Borrelli, P., Robinson, D.A., Fleischer, L.R., Lugato, E., Ballabio, C., Alewell, C. et al. (2017) An assessment of the global impact of 21st century land use change on soil erosion. *Nature Communications*, 8(1), 2013. <https://doi.org/10.1038/s41467-017-02142-7>
- Borrelli, P., Robinson, D.A., Panagos, P., Lugato, E., Yang, J.E., Alewell, C. et al. (2020) Land use and climate change impacts on global soil erosion by water (2015–2070). *Proceedings of the National Academy of Sciences*, 117, 21994–22001.
- Christensen, B.T., Olesen, J.E., Hansen, E.M. & Thomsen, I.K. (2011) Annual variation in  $\delta^{13}\text{C}$  values of maize and wheat: Effect on estimates of decadal scale soil carbon turnover. *Soil Biology and Biochemistry*, 43(9), 1961–1967. <https://doi.org/10.1016/j.soilbio.2011.06.008>
- Cobo, J.G., Dercon, G. & Cadisch, G. (2010) Nutrient balances in African land use systems across different spatial scales: a review of approaches, challenges and progress. *Agriculture, Ecosystems & Environment*, 136(1-2), 1–15. <https://doi.org/10.1016/j.agee.2009.11.006>
- Collins, A., Walling, D. & Ls, G. (1997) Use of the geochemical record preserved in floodplain deposits to reconstruct recent changes in river basin sediment sources. *Geomorphology*, 19(1-2), 151–167. [https://doi.org/10.1016/S0169-555X\(96\)00044-X](https://doi.org/10.1016/S0169-555X(96)00044-X)
- Conte, C.A. (1999) The forest becomes desert: Forest use and environmental change in Tanzania's West Usambara mountains. *Land Degradation & Development*, 10(4), 291–309. [https://doi.org/10.1002/\(SICI\)1099-145X\(199907/08\)10:4<291::AID-LDR363>3.0.CO;2-W](https://doi.org/10.1002/(SICI)1099-145X(199907/08)10:4<291::AID-LDR363>3.0.CO;2-W)
- Deus, D., Gloaguen, R. & Krause, P. (2013) Water balance modeling in a semi-arid environment with limited in situ data using remote sensing in Lake Manyara, East African Rift, Tanzania. *Remote Sensing*, 5(4), 1651–1680. <https://doi.org/10.3390/rs5041651>
- D'haen, K., Verstraeten, G. & Degryse, P. (2012) Fingerprinting historical fluvial sediment fluxes. *Progress in Physical Geography*, 36(2), 154–186. <https://doi.org/10.1177/0309133311432581>
- Du, P. & Walling, D. (2012) Using 210Pb measurements to estimate sedimentation rates on river floodplains. *Journal of Environmental Radioactivity*, 103(1), 59–75. <https://doi.org/10.1016/j.jenvrad.2011.08.006>
- Du, P. & Walling, D.E. (2017) Fingerprinting surficial sediment sources: Exploring some potential problems associated with the spatial variability of source material properties. *Journal of Environmental Management*, 194, 4–15. <https://doi.org/10.1016/j.jenvman.2016.05.066>
- Dutton, C.L., Subalasky, A.L., Hill, T.D., Aleman, J.C., Rosi, E.J., Onyango, K. B. et al. (2019) A 2000-year sediment record reveals rapidly changing sedimentation and land use since the 1960s in the Upper Mara-Serengeti Ecosystem. *Science of the Total Environment*, 664, 148–160. <https://doi.org/10.1016/j.scitotenv.2019.01.421>
- FAO. (2019) *FAOSTAT statistical database*. Rome: Food and Agriculture Organization of the United Nations.
- Guzha, A., Rufino, M., Okoth, S., Jacobs, S. & Nóbrega, R. (2018) Impacts of land use and land cover change on surface runoff, discharge and low flows: Evidence from East Africa. *Journal of Hydrology: Regional Studies*, 15, 49–67.
- He, Q. & Walling, D. (1997) The distribution of fallout 137Cs and 210Pb in undisturbed and cultivated soils. *Applied Radiation and Isotopes*, 48(5), 677–690. [https://doi.org/10.1016/S0969-8043\(96\)00302-8](https://doi.org/10.1016/S0969-8043(96)00302-8)
- Hughes, A.O., Olley, J.M., Croke, J.C. & Mckergow, L.A. (2009) Sediment source changes over the last 250 years in a dry-tropical catchment, central Queensland, Australia. *Geomorphology*, 104(3-4), 262–275. <https://doi.org/10.1016/j.geomorph.2008.09.003>
- Jacobs, S.R., Timbe, E., Weeser, B., Rufino, M.C., Butterbach-Bahl, K. & Breuer, L. (2018) Assessment of hydrological pathways in East African montane catchments under different land use. *Hydrology and Earth System Sciences*, 22(9), 4981–5000. <https://doi.org/10.5194/hess-22-4981-2018>
- Janssens de Bisthoven, L., Vanhove, M.P.M., Rochette, A.J., Hugé, J., Verbesselt, S., Machunda, R. et al. (2020) Social-ecological assessment of Lake Manyara basin, Tanzania: A mixed method approach. *Journal of Environmental Management*, 267, 110594. <https://doi.org/10.1016/j.jenvman.2020.110594>
- Jones, B. & Deocampo, D. (2003) Geochemistry of saline lakes. *Treatise on Geochemistry*, 5, 605.
- Kelly, C., Wynants, M., Munishi, L.K., Nasser, M., Patrick, A., Mtei, K.M. et al. (2020) 'Mind the Gap': Reconnecting local actions and multi-level policies to bridge the governance gap. An example of soil erosion action from East Africa. *Landscape*, 9, 352.
- Kiagi, L.M. (2013) Perspectives on the assumed causes of land degradation in the rangelands of Sub-Saharan Africa. *Progress in Physical*

- Geography*, 37(5), 664–684. <https://doi.org/10.1177/0309133313492543>
- Kiunsi, R. & Meadows, M. (2006) Assessing land degradation in the Monduli District, northern Tanzania. *Land Degradation & Development*, 17(5), 509–525. <https://doi.org/10.1002/ldr.733>
- Lacey, J.P., Evrard, O., Smith, H.G., Blake, W.H., Olley, J.M., Minella, J. P. & Owens, P.N. (2017) The challenges and opportunities of addressing particle size effects in sediment source fingerprinting: A review. *Earth-Science Reviews*, 169, 85–103. <https://doi.org/10.1016/j.earscirev.2017.04.009>
- Lizaga, I., Bodé, S., Gaspar, L., Latorre, B., Boeckx, P. & Navas, A. (2021) Legacy of historic land cover changes on sediment provenance tracked with isotopic tracers in a Mediterranean agroforestry catchment. *Journal of Environmental Management*, 288, 112291. <https://doi.org/10.1016/j.jenvman.2021.112291>
- Lizaga, I., Gaspar, L., Blake, W.H., Latorre, B. & Navas, A. (2019) Fingerprinting changes of source apportionments from mixed land uses in stream sediments before and after an exceptional rainstorm event. *Geomorphology*, 341, 216–229. <https://doi.org/10.1016/j.geomorph.2019.05.015>
- Łokas, E., Wachniew, P., Ciszewski, D., Owczarek, P. & Chau, N.D. (2010) Simultaneous use of trace metals, 210Pb and 137Cs in floodplain sediments of a lowland river as indicators of anthropogenic impacts. *Water, Air, and Soil Pollution*, 207(1–4), 57–71. <https://doi.org/10.1007/s11270-009-0119-4>
- Mabit, L., Benmansour, M. & Walling, D. (2008) Comparative advantages and limitations of the fallout radionuclides 137Cs, 210Pbex and 7Be for assessing soil erosion and sedimentation. *Journal of Environmental Radioactivity*, 99(12), 1799–1807. <https://doi.org/10.1016/j.jenvrad.2008.08.009>
- Maerker, M., Quénéhervé, G., Bachofer, F. & Mori, S. (2015) A simple DEM assessment procedure for gully system analysis in the Lake Manyara area, northern Tanzania. *Natural Hazards*, 79(S1), 235–253. <https://doi.org/10.1007/s11069-015-1855-y>
- Maitima, J.M., Mugatha, S.M., Reid, R.S., Gachimbi, L.N., Majule, A., Lyaruu, H. et al. (2009) The linkages between land use change, land degradation and biodiversity across East Africa. *African Journal of Environmental Science and Technology*, 3(10), 310–325.
- Manjoro, M., Rowntree, K., Kakembo, V., Foster, I. & Collins, A.L. (2017) Use of sediment source fingerprinting to assess the role of subsurface erosion in the supply of fine sediment in a degraded catchment in the Eastern Cape, South Africa. *Journal of Environmental Management*, 194, 27–41. <https://doi.org/10.1016/j.jenvman.2016.07.019>
- Motha, J., Wallbrink, P., Hairsine, P. & Grayson, R. (2002) Tracer properties of eroded sediment and source material. *Hydrological Processes*, 16(10), 1983–2000. <https://doi.org/10.1002/hyp.397>
- Ngecu, W. & Mathu, E. (1999) The El-Nino-triggered landslides and their socioeconomic impact on Kenya. *Environmental Geology*, 38(4), 277–284. <https://doi.org/10.1007/s002540050425>
- Nicholson, S.E. (1996) A review of climate dynamics and climate variability in Eastern Africa. In: Johnson, T.C. & Odada, E.O. (Eds.) *The limnology, climatology and paleoclimatology of the East African lakes*. Amsterdam: Gordon and Breach Publishers.
- Olago, D.O. & Odada, E.O. (2007) Sediment impacts in Africa's trans-boundary lake/river basins: Case study of the East African Great Lakes. *Aquatic Ecosystem Health & Management*, 10(1), 23–32. <https://doi.org/10.1080/14634980701223727>
- Osborne, C.P. (2008) Atmosphere, ecology and evolution: what drove the Miocene expansion of C4 grasslands? *Journal of Ecology*, 96, 35–45.
- Outridge, P.M. & Wang, F. (2015) *The stability of metal profiles in freshwater and marine sediments*. Environmental Contaminants. Dordrecht: Springer.
- Owens, P., Blake, W., Gaspar, L., Gateuille, D., Koiter, A., Lobb, D. et al. (2016) Fingerprinting and tracing the sources of soils and sediments: Earth and ocean science, geoarchaeological, forensic, and human health applications. *Earth-Science Reviews*, 162, 1–23. <https://doi.org/10.1016/j.earscirev.2016.08.012>
- Poesen, J., Nachtergaele, J., Verstraeten, G. & Valentin, C. (2003) Gully erosion and environmental change: Importance and research needs. *Catena*, 50(2–4), 91–133. [https://doi.org/10.1016/S0341-8162\(02\)00143-1](https://doi.org/10.1016/S0341-8162(02)00143-1)
- Prins, H. & Loth, P. (1988) Rainfall patterns as background to plant phenology in northern Tanzania. *Journal of Biogeography*, 15(3), 451–463. <https://doi.org/10.2307/2845275>
- Rabinovich, A., Heath, S.C., Zhischenko, V., Mkilema, F., Patrick, A., Nasser, M. et al. (2020) Protecting the commons: Predictors of willingness to mitigate communal land degradation among Maasai pastoralists. *Journal of Environmental Psychology*, 72, 101504.
- Rabinovich, A., Kelly, C., Wilson, G., Nasser, M., Ngondya, I., Patrick, A. et al. (2019) “We will change whether we want it or not”: Soil erosion in Maasai land as a social dilemma and a challenge to community resilience. *Journal of Environmental Psychology*, 66, 101365. <https://doi.org/10.1016/j.jenvp.2019.101365>
- Rapp, A., Murray-Rust, D.H., Christiansson, C. & Berry, L. (1972) Soil erosion and sedimentation in four catchments near Dodoma, Tanzania. *Geografiska Annaler. Series A. Physical Geography*, 54(3–4), 255–318. <https://doi.org/10.1080/04353676.1972.11879870>
- Salami, A., Kamara, A.B. & Brixiova, Z. (2010) *Smallholder agriculture in East Africa: Trends, constraints and opportunities*. Tunis: African Development Bank.
- Sanchez, P.A. (2002) Soil fertility and hunger in Africa. *Science*, 295(5562), 2019–2020. <https://doi.org/10.1126/science.1065256>
- Sanchez-Cabeza, J. & Ruiz-Fernández, A. (2012) 210Pb sediment radiochronology: An integrated formulation and classification of dating models. *Geochimica et Cosmochimica Acta*, 82, 183–200. <https://doi.org/10.1016/j.gca.2010.12.024>
- Schillereff, D.N., Chiverrell, R.C., MacDonald, N. & Hooke, J.M. (2014) Flood stratigraphies in lake sediments: A review. *Earth-Science Reviews*, 135, 17–37. <https://doi.org/10.1016/j.earscirev.2014.03.011>
- Sherriff, S.C., Franks, S.W., Rowan, J.S., Fenton, O. & Óhuallacháin, D. (2015) Uncertainty-based assessment of tracer selection, tracer non-conservativeness and multiple solutions in sediment fingerprinting using synthetic and field data. *Journal of Soils and Sediments*, 15, 2101–2116.
- Shongwe, M.E., Van Oldenborgh, G.J., Van Den Hurk, B. & Van Aalst, M. (2011) Projected changes in mean and extreme precipitation in Africa under global warming. Part II: East Africa. *Journal of Climate*, 24, 3718–3733.
- Tengberg, A. & Stocking, M. (1997) *Erosion-induced loss in soil productivity and its impacts on agricultural production and food security*. Harare, Zimbabwe: FAO/AGRITEX Expert Consultation on Integrated Soil Management for Sustainable Agriculture and Food Security in Southern and Eastern Africa, pp. 8–12.
- UNDESA. (2017) Population Division – World Population Prospects. In: Division, U.N.P. (Ed.) *The 2017 review*. New York, US.: UNDESA.
- Upadhayay, H.R., Griepentrog, M., Bodé, S., Bajracharya, R.M., Cornelis, W., Collins, A.L. & Boeckx, P. (2020) Catchment-wide variations and biogeochemical time lags in soil fatty acid carbon isotope composition for different land uses: Implications for sediment source classification. *Organic Geochemistry*, 146, 104048. <https://doi.org/10.1016/j.orggeochem.2020.104048>
- Vanmaercke, M., Poesen, J., Broeckx, J. & Nyssen, J. (2014) Sediment yield in Africa. *Earth-Science Reviews*, 136, 350–368. <https://doi.org/10.1016/j.earscirev.2014.06.004>
- Walling, D.E. (2013) The evolution of sediment source fingerprinting investigations in fluvial systems. *Journal of Soils and Sediments*, 13(10), 1658–1675. <https://doi.org/10.1007/s11368-013-0767-2>
- Walling, D. & He, Q. (2000) The global distribution of bomb-derived 137Cs reference inventories. *Final Report on IAEA Technical Contract*, 10361, 1–11.
- Wynants, M., Kelly, C., Mtei, K., Munishi, L., Patrick, A., Rabinovich, A. et al. (2019) Drivers of increased soil erosion in East Africa's agro-pastoral systems: changing interactions between the social, economic and natural domains. *Regional Environmental Change*, 19, 1902–1921.
- Wynants, M., Millward, G., Patrick, A., Taylor, A., Munishi, L., Mtei, K. et al. (2020) Determining tributary sources of increased sedimentation in

- East-African Rift Lakes. *Science of the Total Environment*, 717, 137266. <https://doi.org/10.1016/j.scitotenv.2020.137266>
- Wynants, M., Munishi, L., Mtei, K., Bodé, S., Patrick, A., Taylor, A. et al. (2021) Soil erosion and sediment transport in Tanzania: Part I – sediment source tracing in three neighbouring river catchments. *Earth Surface Processes and Landforms*.
- Wynants, M., Solomon, H., Ndakidemi, P. & Blake, W.H. (2018) Pinpointing areas of increased soil erosion risk following land cover change in the Lake Manyara catchment, Tanzania. *International Journal of Applied Earth Observation and Geoinformation*, 71, 1–8. <https://doi.org/10.1016/j.jag.2018.05.008>
- Zaborska, A., Carroll, J., Papucci, C. & Pempkowiak, J. (2007) Intercomparison of alpha and gamma spectrometry techniques used in <sup>210</sup>Pb geochronology. *Journal of Environmental Radioactivity*, 93(1), 38–50. <https://doi.org/10.1016/j.jenvrad.2006.11.007>

## SUPPORTING INFORMATION

Additional supporting information may be found in the online version of the article at the publisher's website.

**How to cite this article:** Wynants, M., Patrick, A., Munishi, L., Mtei, K., Bodé, S., Taylor, A. et al. (2021) Soil erosion and sediment transport in Tanzania: Part II – sedimentological evidence of phased land degradation. *Earth Surface Processes and Landforms*, 1–15. Available from: <https://doi.org/10.1002/esp.5218>